GEOLOGY | THE GEOLOGICAL SOCIETY OF AMERICA®

Stable tungsten isotopic composition of seawater over the past 80 million years

Ruiyu Yang[1,2,3], Daniel Stubbs[4], Tim Elliott[4], Tao Li[5], Tianyu Chen[1], Adina Paytan[6], David B. Kemp[7], Hongfei Ling[1], Jun Chen[1], James R. Hein[8], Christopher D. Coath[4], and Gaojun Li[1,*]

[1]Department of Earth and Planetary Sciences, Nanjing University, Nanjing 210023, China
[2]Institute of Geology and Mineralogy, University of Cologne, Cologne 50674, Germany
[3]GEOMAR Helmholtz Centre for Ocean Research, Kiel 24148, Germany
[4]School of Earth Sciences, University of Bristol, Bristol BS8 1RJ, UK
[5]State Key Laboratory of Palaeobiology and Stratigraphy, Nanjing Institute of Geology and Palaeontology, Nanjing 210008, China
[6]Institute of Marine Sciences, University of California, Santa Cruz, California 95064, USA
[7]State Key Laboratory of Biogeology and Hubei Key Laboratory of Critical Zone Evolution, School of Earth Sciences,
 China University of Geosciences, Wuhan 430074, China
[8]U.S. Geological Survey (retired), Santa Cruz, California 95060, USA

ABSTRACT

The isotopic composition of seawater provides valuable information on how the Earth system has evolved. Here we present the stable tungsten isotopic composition ($\delta^{186/184}$W) of seawater recorded in three ferromanganese (Fe-Mn) crusts spanning the past 80 million years in the Pacific. The $\delta^{186/184}$W of Fe-Mn crusts displays a pronounced decrease of ∼0.2‰ from 60 Ma to 40 Ma followed by a stable value of ∼0‰ since ca. 40 Ma. Multiple lines of evidence indicate an invariable equilibrium isotopic fractionation between Fe-Mn crusts and seawater. The consistent variations in $\delta^{186/184}$W in the three Fe-Mn crusts also indicate limited alteration by deposition regime or diagenetic overprinting. Thus, the $\delta^{186/184}$W of Fe-Mn crusts reflects mainly that of seawater. A simple mass-balance calculation and comparison to other proxies suggest that the early Cenozoic decrease of seawater $\delta^{186/184}$W was most likely caused by decreased W isotopic fractionation between seawater and W sinks linked to shifting sedimentation regimes. We propose that increased burial of organics and decreased Fe-Mn oxide (FMO) sedimentation may result in a smaller isotopic fractionation associated with W sinks by limiting the adsorption of W from the water column onto FMOs in open-ocean sediments. Our results demonstrate the potential of $\delta^{186/184}$W as a novel paleo-proxy for global biogeochemical cycling.

INTRODUCTION

Much of the information on how the Earth system has evolved relies on records of the isotopic compositions of various elements in seawater. Great efforts have been made to develop new isotopic proxies for different aspects of the global biogeochemical cycles (e.g., Teng et al., 2017, and references therein). The stable W isotopes ($\delta^{186/184}$W) have great potential for paleoenvironmental reconstruction because W cycling is linked to redox-sensitive elements such as S and Fe (Dellwig et al., 2019; Kurzweil et al., 2021). Recent advances in the understanding of the behavior of stable W isotopes at Earth's surface have helped to constrain the oceanic budget of W (Fujiwara et al., 2020; Kashiwabara et al., 2017; Kurzweil et al., 2021; Yang et al., 2022). However, continuous records of the long-term evolution of seawater $\delta^{186/184}$W are still lacking (e.g., Alam et al., 2022; Roué et al., 2021; Tsujisaka et al., 2020).

This work reports a record of seawater $\delta^{186/184}$W spanning the past 80 m.y. documented in three ferromanganese (Fe-Mn) crusts in the Pacific Ocean (Fig. S1 in the Supplemental Material[1]). The strong affinity and thus low diffusion rate of W in Fe-Mn oxides (FMOs) (Henderson and Burton, 1999) make Fe-Mn crusts a potentially excellent archive for preserving seawater $\delta^{186/184}$W. The availability of well-preserved archives documenting changes in seawater chemistry and environmental conditions for the past ∼80 m.y. also offers a unique opportunity to explore the likely processes that controlled seawater $\delta^{186/184}$W.

MATERIALS AND METHODS

Three Fe-Mn crusts from the Pacific (Fig. S1) were chosen for $\delta^{186/184}$W analysis. Crusts MDD53 and CJ01 are both hydrogenetic and recovered from seamounts in the northwestern Pacific Ocean. Crust MDD53 was collected near the Mariana arc (17°26′34″N, 150°17′18″E, 2700 m water depth) (Chen et al., 2013). Crust CJ01 was collected at a site (17°59′18″N, 177°42′34″W, 3082 m water depth) 3386 km to the east of crust MDD53 (Ling et al., 2005). Crust CJ01 shows no phosphatization, while MDD53 shows slight phosphatization in its oldest part. A third crust, Yaloc, was collected near the East Pacific Rise in the Bauer Basin, southeastern Pacific (13°40′48″S, 102°08′06″W, 4435–4214 m water depth) (van de Flierdt et al., 2004). The Yaloc crust experienced two hydrothermal periods with a supply of metals identified by Pb isotopes at ca. 6.5 Ma and 4.4–2.9 Ma (van de Flierdt et al., 2004).
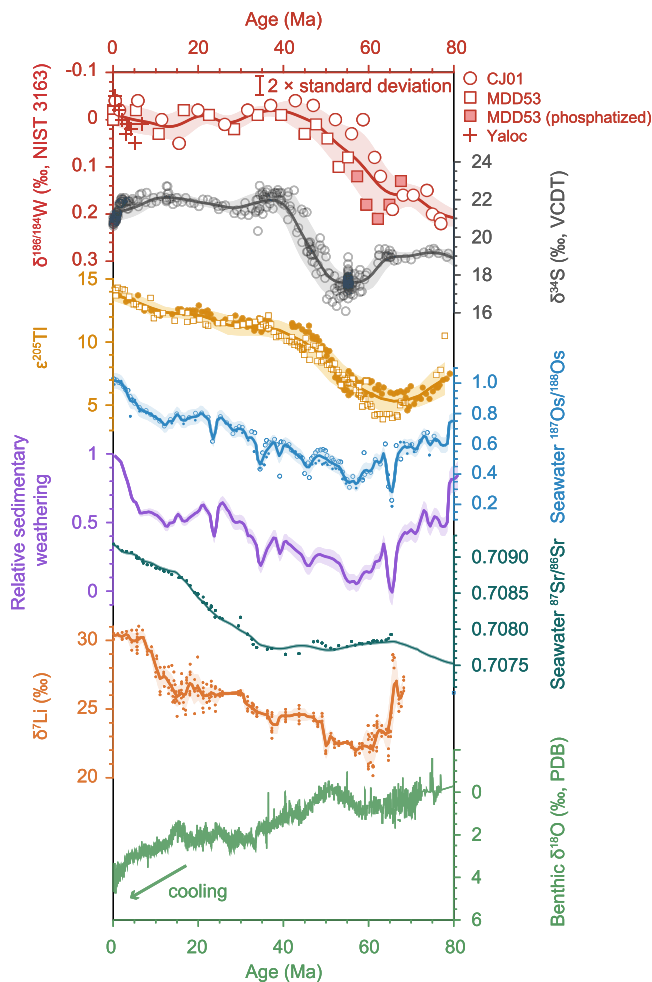
Gaojun Li https://orcid.org/0000-0002-2463-0774
*ligaojun@nju.edu.cn

Figure 1. δ186/184W records (with reversed axis; relative to standard reference material NIST 3163) of Fe-Mn crusts CJ01, MDD53, and Yaloc over the past 80 m.y. compared with marine barite δ34S (relative to Vienna Canyon Diablo troilite [VCDT]; Yao et al., 2020), ε205Tl (Nielsen et al., 2009), 187Os/188Os (Burton, 2006; Klemm et al., 2005), relative sedimentary weathering based on a model (Li and Elderfield, 2013), 87Sr/86Sr (McArthur et al., 2001), δ7Li (Misra and Froelich, 2012) (adjusted to match modern seawater), and benthic δ18O (relative to Peedee belemnite [PDB] to represent bottom sea temperature; Cramer et al., 2009; Westerhold et al., 2020). Solid red squares represent the phosphatized sub-samples of MDD53 (Hu et al., 2012). The δ186/184W, δ34S, and ε205Tl records were smoothed with a width of 3 m.y., and the other records were smoothed with a width of 0.5 m.y. Shaded error envelopes for each isotopic record are 2 × standard error of the mean.

The two hydrogenetic crusts (MDD53 and CJ01) span the whole Cenozoic and the Late Cretaceous, according to the empirical relationship between growth rate and Co content. Although the uncertainty of the Co age model could be roughly 10% (Frank et al., 1999) (Fig. S4), similar Pb isotope variations in both crusts, along with those of eolian deposits from core LL44-GPC3 in the central North Pacific, confirm the fidelity of Co age models (Chen et al., 2013; Ling et al., 2005). The chronology of the younger Fe-Mn crust, Yaloc (7.1 Ma), is based on the decay of 10Be (van de Flierdt et al., 2004). Details for sample pretreatment and stable W isotopic analyses can be found in the Supplemental Material.

RESULTS

The Fe-Mn crusts analyzed in this study show high W concentrations (42–134 μg g^{-1}), which are 20–70 times higher than those of the average upper continental crust. The three crusts show similar δ186/184W values within analytical uncertainty across overlapping time intervals (Fig. 1; Table S1 in the Supplemental Material) despite differences in deposition regimes (mixed hydrogenetic-hydrothermal versus hydrogenetic), location, water depth, and degree of diagenetic alteration. The δ186/184W variability of the Fe-Mn crusts (−0.05‰ to ~0.23‰) exceeds the analytical reproducibility (0.04‰, ± 2 × external standard deviation) by more than a factor of 5. We see an offset of ~0.58‰ in δ186/184W between the most recent Fe-Mn crust layers (−0.04‰ ± 0.02‰) and modern seawater (0.54‰ ± 0.05‰; Kurzweil et al., 2021). The δ186/184W values of the Fe-Mn crusts show a gradual shift of ~0.20‰ from ca. 60 Ma to ca. 40 Ma, followed by relatively constant values (~0.00‰) through the rest of the Cenozoic (Fig. 1).

DISCUSSION
Fe-Mn Crusts as Archives of Seawater δ186/184W

The high W concentrations in Fe-Mn crusts (42–134 μg g^{-1}) compared to that of seawater (9 × 10^{-6} μg g^{-1}) (Firdaus et al., 2008; Kurzweil et al., 2021) reflect high affinity of W in Fe-Mn crusts. The mixed hydrogenetic-hydrothermal crust Yaloc shows no sign of abnormally high concentrations of W or anomalous δ186/184W values during intervals of known hydrothermal activity (Fig. S2). Thus, we conclude that W in all three analyzed Fe-Mn crusts is primarily of hydrogenetic origin.

The comparable δ186/184W values of crusts from different locations are consistent with the homogeneity of the seawater δ186/184W (Fujiwara et al., 2020; Kurzweil et al., 2021). Although the residence time of W in seawater (~4 k.y.; Yang et al., 2022) is not as long as that of most other conservative elements, it may still be long enough to homogenize δ186/184W in major oceans due to the non-nutrient behavior of W (Firdaus et al., 2008). The most likely diagenetic process that could alter the original δ186/184W signals is phosphatization. However, the consistent δ186/184W values of crusts CJ01 (non-phosphatized) and MDD53 (mildly phosphatized in its oldest part; Fig. 1) suggest a limited influence of post-depositional diagenetic overprinting on the δ186/184W of Fe-Mn crusts. An extremely low diffusion coefficient of 3.64 × 10^{-10} cm^2 yr^{-1} can be calculated for W in the Fe-Mn crusts based on the ratio of W concentrations (1.1 × 10^7) in Fe-Mn crusts and seawater (Henderson and Burton, 1999). The low diffusion coefficient indicates that W diffusion in Fe-Mn crusts is <1.6 mm in 80 m.y., suggesting limited diffusive alteration after deposition.

The offset of δ186/184W (~0.58‰) between the most recent Fe-Mn crust layers and modern seawater is consistent with experimentally predicted equilibrium isotope fractionation associated with the adsorption of dissolved WO_4^{2-} onto FMOs (δ186/184W$_{dissolved}$ − δ186/184W$_{adsorbed}$ = 0.50‰ ± 0.06‰ for ferrihydrite and 0.58‰ ± 0.14‰ for birnessite [δ-MnO_2]) (Kashiwabara et al., 2017), arguing for a possible equilibrium isotopic fractionation. The slight difference (~0.08‰) in W isotopic fractionations associated with precipitation from seawater between the Fe and Mn oxyhydroxides (Kashiwabara et al., 2017) also explains the lack of correlation between mineralogy (as reflected by Mn/Fe) and δ186/184W (Fig. S3). The consistent δ186/184W values of the surface sections of the three crusts formed under different depositional regimes (hydrogenetic versus mixed hydrogenetic-hydrothermal) and growth rates (0.9–15.8 mm m.y.$^{-1}$) also suggest that the Fe-Mn crusts likely maintained W isotopic equilibrium with seawater. Additionally, despite the dramatic changes in bottom sea temperature during the late Cenozoic (Fig. 1), the Fe-Mn crust δ186/184W remained relatively unchanged, indicating low sensitivity of W isotopic fractionation to temperature fluctuations. Taken together, the evidence listed above indicates that Fe-Mn crusts can provide robust temporal records of seawater δ186/184W.

Controls on the Evolution of Seawater δ186/184W

Recent investigations of W isotope systematics in Earth's surface materials (Yang et al., 2022) show that rivers are the main carriers
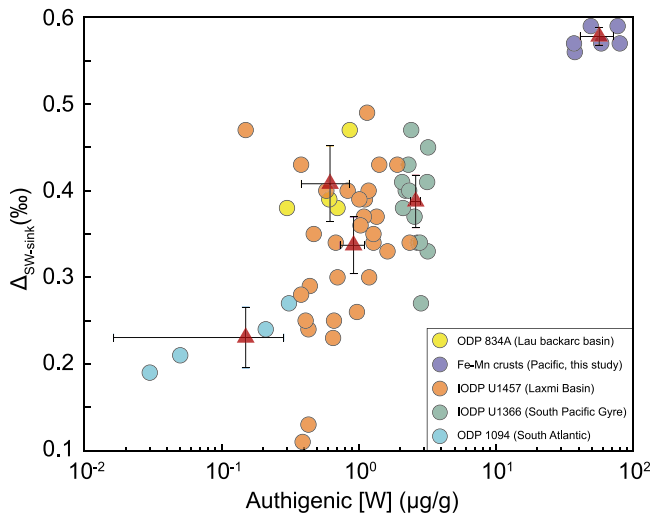
Figure 2. $\Delta_{SW-sink}$ (overall isotopic fractionation between seawater and W sinks) values associated with sedimentary W sinks against authigenic W concentrations. Data sources of these values are listed in Table S2 (see text footnote 1) and include Ocean Drilling Program Site (ODP) 834A (clayey nannofossil ooze), International Ocean Discovery Program (IODP) Site U1457 (nannofossil ooze, clay, and sand), IODP Site U1366 (zeolitic metalliferous pelagic clay), and ODP Site 1094 (mud-bearing diatom ooze). Red triangles represent the mean values of each group, with error bars showing two standard errors of the mean. Additional information regarding the calculation methods of $\Delta_{SW-sink}$ can be found in the Supplemental Material.
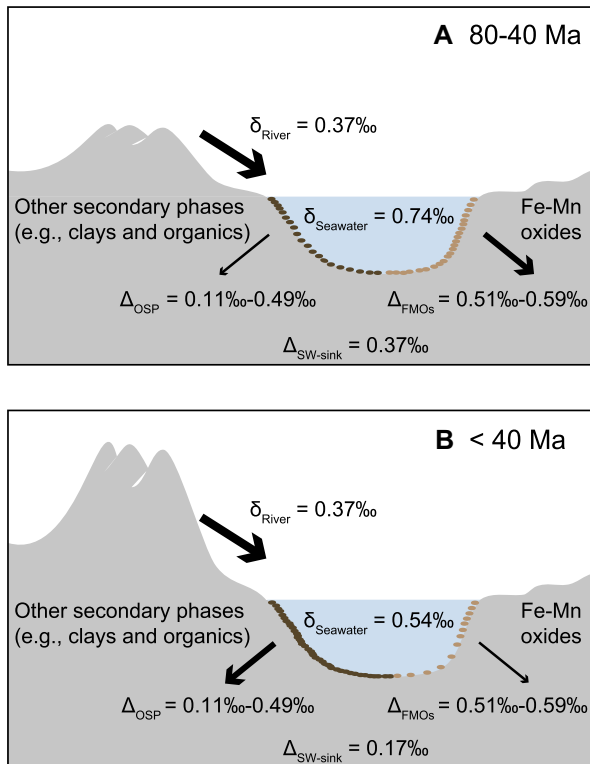
of W to the ocean. The main sink of W from seawater is associated with non-euxinic sediments, including FMOs, clay minerals, organics, and other authigenic minerals (Kashiwabara et al., 2017; Sen Tuna and Braida, 2014). The altered oceanic crust may not act as a primary

sink for seawater-derived W (Reifenröther et al., 2022). On million-year time scales, the steady-state $\delta^{186/184}$W of seawater is determined by the $\delta^{186/184}$W of riverine input and the overall isotopic fractionation between seawater and W sinks ($\Delta_{SW-sink}$) (Yang et al., 2022):

$$\delta^{186/184}W_{seawater} = \delta^{186/184}W_{river} + \Delta_{SW-sink}. \quad (1)$$

The present-day $\delta^{186/184}$W of riverine inputs estimated by major rivers in Asia is 0.37‰ ± 0.04‰, which is heavier than that of the weathered upper continental crust (0.01‰ ± 0.01‰) due to the preferential uptake of lighter W isotopes by secondary precipitates such as FMOs and clay minerals in the regolith (Yang et al., 2022). The $\delta^{186/184}$W of the riverine input is likely controlled by lithology of the weathered rocks. A higher contribution of sedimentary rocks relative to crystalline silicates is associated with lower $\delta^{186/184}$W values and higher W concentrations in river water (Yang et al., 2022). Based on Equation 1, assuming a constant $\Delta_{SW-sink}$, a decreasing seawater $\delta^{186/184}$W could be caused by a decline in riverine $\delta^{186/184}$W, which possibly reflects an increased contribution of sedimentary rock weathering. However, the observed evolution of seawater $\delta^{186/184}$W doesn't align with expected lithological changes of weathered rocks seen in other proxies such as Os, Li, and Sr isotopes (Fig. 1). Seawater ^{187}Os/^{188}Os, which is controlled largely by weathering of organic-rich sedimentary rocks with high ^{187}Os/^{188}Os, sug-
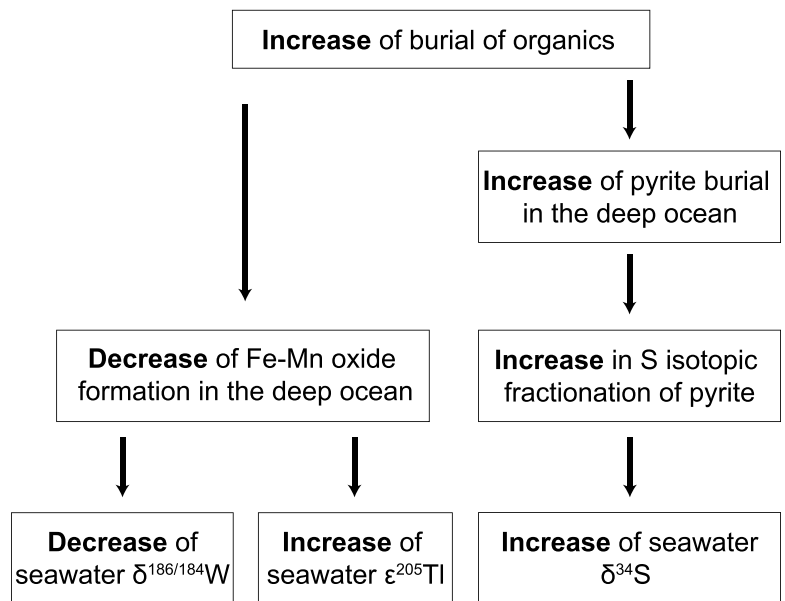

Figure 3. Evolution of the $\delta^{186/184}$W ocean budget over the past 80 m.y. illustrated through cartoons and a flowchart. Contributions from hydrothermal flux, benthic fluxes, and altered oceanic crust are neglected due to their minor impact. (A, B) W budgets in Late Cretaceous to early Cenozoic (80–40 Ma) ocean (A) and later Cenozoic (<40 Ma) ocean (B) are attributed to variations in W burial with distinct $\Delta_{SW-sink}$ (the overall isotopic fractionation between seawater and W sinks). Δ_{FMOs} is the isotopic fractionation between seawater and Fe-Mn oxides (FMOs), while Δ_{OSP} is the isotopic fractionation between seawater and other secondary phases. δ_{River} and $\delta_{Seawater}$ are $\delta^{186/184}$W compositions of riverine input and seawater. Size of arrows denotes estimated flux of each end member. (C) Potential mechanism elucidating concomitant evolution of seawater $\delta^{186/184}$W, ε^{205}Tl, and δ^{34}S in the early Cenozoic.

gests a progressive increase in the contribution of sedimentary rock weathering during the Cenozoic (Ravizza and Peucker-Ehrenbrink, 2003). The inverse calculation based on C, Sr, and Os isotopic records (Li and Elderfield, 2013) indicates that relative sedimentary weathering decreased from ca. 80 Ma to ca. 57 Ma, and then increased for the rest of the Cenozoic (Fig. 1). Seawater δ^7Li is generally inferred to reflect weathering processes, although the precise mechanisms remain a topic of discussion (e.g., Caves Rugenstein et al., 2019; Misra and Froelich, 2012). Considering age uncertainty (Fig. S4), the $\delta^{186/184}$W decline during ca. 60–40 Ma may be aligned with the increasing ^{187}Os/^{188}Os, calculated relative sedimentary weathering and δ^7Li (Fig. 1). Nonetheless, the stability of $\delta^{186/184}$W since 40 Ma is incongruous with the evidence presented by these weathering indicators. Therefore, changes in riverine input cannot fully explain the evolution of seawater $\delta^{186/184}$W over the past 80 m.y.

An alternative scenario for the early Cenozoic decrease in seawater $\delta^{186/184}$W might be a decreasing $\Delta_{SW-sink}$. A compilation of marine sediments (including siliceous, calcareous, and metalliferous sediments and Fe-Mn crusts; Table S2) shows large variability in $\Delta_{SW-sink}$ between 0.11‰ and 0.59‰ (Fig. 2). The equilibrium W isotopic fractionation offset associated with the uptake by FMOs (0.51‰–0.59‰) (Kashiwabara et al., 2017) is much higher than that of most of the sedimentary sinks (Fig. 2). Given the limited laboratory and sedimentary data, precise fractionation factors for individual sinks cannot be defined at present. To simplify our calculation, we conceptually split the non-euxinic sedimentary sinks into two end members, namely, FMOs with higher fractionation of 0.51‰–0.59‰, and all other secondary phases (e.g., clay minerals and organics) with lower fractionation of 0.11‰–0.49‰. Thus, the larger the W sink associated with FMOs, the higher $\Delta_{SW-sink}$ would be (Fig. 2).

We propose that the early Cenozoic shift in seawater $\delta^{186/184}$W was a result of a decrease in $\Delta_{SW-sink}$ in response to a decrease in the proportion of W sink associated with FMOs. Evidence may be found in the seawater δ^{34}S and ε^{205}Tl records, which show a remarkable increase in the early Cenozoic followed by a period without dramatic changes (e.g., Nielsen et al., 2009; Yao et al., 2020; Fig. 1). Pyrite burial is a key factor controlling seawater δ^{34}S, although the riverine and volcanic sulfur input to the ocean also have impacts (Yao and Paytan, 2020, and references therein). Seawater $\delta^{186/184}$W and ε^{205}Tl are both significantly modulated by adsorption of FMOs (Kurzweil et al., 2021; Nielsen et al., 2009). The ubiquitous precipitation of FMOs is driven primarily by the availability of Fe and Mn in the water column, which is low because

large portions of Fe and Mn are utilized biologically and buried with organics (Tagliabue et al., 2017). Assuming a constant flux of Fe and Mn into the ocean, increased organics burial would decrease the availability of Fe and Mn in the water column and further decrease the chemical sedimentation of FMOs. The burial of organics and pyrite are typically interrelated (Berner, 1984). Increased organics and thus pyrite burial would lead to a decrease in seawater δ^{34}S (Kurtz et al., 2003). This would also reduce the adsorption of W and Tl onto FMOs, which would alter their isotopic compositions in seawater (Kurzweil et al., 2022; Nielsen et al., 2009) (Fig. 3). Notably, the increase in seawater δ^{34}S occurred later than the shifts in $\delta^{186/184}$W and ε^{205}Tl records in the early Cenozoic (Fig. 1). Input of lighter δ^{34}S from outgassing in the North Atlantic Igneous Province (63–50 Ma) (Laakso et al., 2020) may have masked the impact of increased burial of organics on seawater δ^{34}S, thereby elucidating the observed offset.

CONCLUSIONS

This study presents stable W isotopic evolution of seawater for the past 80 m.y. as recorded by three Fe-Mn crusts. Seawater $\delta^{186/184}$W showed a pronounced negative shift of ~0.2‰ during the early Cenozoic. Evaluations of the marine W isotopic budget and the evolution of Earth surface systems as documented by other proxies suggest that this early Cenozoic shift in seawater $\delta^{186/184}$W can be best explained by decreased deposition of Fe-Mn oxides that resulted in lower W isotopic difference between the seawater and overall W sinks. This shifting sedimentation regime that controls the seawater $\delta^{186/184}$W reveals conceivable links between the cycling of W and the redox-sensitive elements S, Fe, and Tl, highlighting the great potential of stable W isotopes for investigating deep-time redox processes and biogeochemical cycling.

REFERENCES CITED
Alam, M., Tripti, M., Gurumurthy, G.P., Sohrin, Y., Tsujisaka, M., Singh, A.D., Takano, S., and Verma, K., 2022, Palaeoredox reconstruction in the eastern Arabian Sea since the late Miocene: Insights from trace elements and stable isotopes of molybdenum ($\delta^{98/95}$Mo) and tungsten ($\delta^{186/184}$W) at IODP Site U1457 of Laxmi Basin: Palaeogeography, Palaeoclimatology, Palaeoecology, v. 587, https://doi.org/10.1016/j.palaeo.2021.110790.

Berner, R.A., 1984, Sedimentary pyrite formation: An update: Geochimica et Cosmochimica Acta, v. 48, p. 605–615, https://doi.org/10.1016/0016-7037(84)90089-9.

Burton, K.W., 2006, Global weathering variations inferred from marine radiogenic isotope records: Journal of Geochemical Exploration, v. 88, p. 262–265, https://doi.org/10.1016/j.gexplo.2005.08.052.

Caves Rugenstein, J.K., Ibarra, D.E., and von Blanckenburg, F., 2019, Neogene cooling driven by land surface reactivity rather than increased weathering fluxes: Nature, v. 571, p. 99–102, https://doi.org/10.1038/s41586-019-1332-y.

Chen, T.Y., Ling, H.F., Hu, R., Frank, M., and Jiang, S.Y., 2013, Lead isotope provinciality of central North Pacific Deep Water over the Cenozoic: Geochemistry, Geophysics, Geosystems, v. 14, p. 1523–1537, https://doi.org/10.1002/ggge.20114.

Cramer, B.S., Toggweiler, J.R., Wright, J.D., Katz, M.E., and Miller, K.G., 2009, Ocean overturning since the Late Cretaceous: Inferences from a new benthic foraminiferal isotope compilation: Paleoceanography, v. 24, PA4216, https://doi.org/10.1029/2008PA001683.

Dellwig, O., Wegwerth, A., Schnetger, B., Schulz, H., and Arz, H.W., 2019, Dissimilar behaviors of the geochemical twins W and Mo in hypoxic-euxinic marine basins: Earth-Science Reviews, v. 193, p. 1–23, https://doi.org/10.1016/j.earscirev.2019.03.017.

Firdaus, M.L., Norisuye, K., Nakagawa, Y., Nakatsuka, S., and Sohrin, Y., 2008, Dissolved and labile particulate Zr, Hf, Nb, Ta, Mo and W in the western North Pacific Ocean: Journal of Oceanography, v. 64, p. 247–257, https://doi.org/10.1007/s10872-008-0019-z.

Frank, M., O'Nions, R.K., Hein, J.R., and Banakar, V.K., 1999, 60 Myr records of major elements and Pb–Nd isotopes from hydrogenous ferromanganese crusts: Reconstruction of seawater paleochemistry: Geochimica et Cosmochimica Acta, v. 63, p. 1689–1708, https://doi.org/10.1016/S0016-7037(99)00079-4.

Fujiwara, Y., Tsujisaka, M., Takano, S., and Sohrin, Y., 2020, Determination of the tungsten isotope composition in seawater: The first vertical profile from the western North Pacific Ocean: Chemical Geology, v. 555, https://doi.org/10.1016/j.chemgeo.2020.119835.

Henderson, G.M., and Burton, K.W., 1999, Using (^{234}U/^{238}U) to assess diffusion rates of isotope tracers in ferromanganese crusts: Earth and Planetary Science Letters, v. 170, p. 169–179, https://doi.org/10.1016/S0012-821X(99)00104-1.

Hu, R., Chen, T.Y., and Ling, H.F., 2012, Late Cenozoic history of deep water circulation in the western North Pacific: Evidence from Nd isotopes of ferromanganese crusts: Chinese Science Bulletin, v. 57, p. 4077–4086, https://doi.org/10.1007/s11434-012-5322-9.

Kashiwabara, T., Kubo, S., Tanaka, M., Senda, R., Iizuka, T., Tanimizu, M., and Takahashi, Y., 2017, Stable isotope fractionation of tungsten during adsorption on Fe and Mn (oxyhydr)oxides: Geochimica et Cosmochimica Acta, v. 204, p. 52–67, https://doi.org/10.1016/j.gca.2017.01.031.

Klemm, V., Levasseur, S., Frank, M., Hein, J.R., and Halliday, A.N., 2005, Osmium isotope stratigraphy of a marine ferromanganese crust: Earth and Planetary Science Letters, v. 238, p. 42–48, https://doi.org/10.1016/j.epsl.2005.07.016.

Kurtz, A.C., Kump, L.R., Arthur, M.A., Zachos, J.C., and Paytan, A., 2003, Early Cenozoic decoupling of the global carbon and sulfur cycles: Paleoceanography, v. 18, 1090, https://doi.org/10.1029/2003PA000908.

Kurzweil, F., Archer, C., Wille, M., Schoenberg, R., Münker, C., and Dellwig, O., 2021, Redox control

on the tungsten isotope composition of seawater: Proceedings of the National Academy of Sciences of the United States of America, v. 118, https://doi.org/10.1073/pnas.2023544118.

Kurzweil, F., Dellwig, O., Wille, M., Schoenberg, R., Arz, H.W., and Münker, C., 2022, The stable tungsten isotope composition of sapropels and manganese-rich sediments from the Baltic Sea: Earth and Planetary Science Letters, v. 578, https://doi.org/10.1016/j.epsl.2021.117303.

Laakso, T.A., Waldeck, A., Macdonald, F.A., and Johnston, D., 2020, Volcanic controls on seawater sulfate over the past 120 million years: Proceedings of the National Academy of Sciences of the United States of America, v. 117, p. 21,118–21,124, https://doi.org/10.1073/pnas.1921308117.

Li, G.J., and Elderfield, H., 2013, Evolution of carbon cycle over the past 100 million years: Geochimica et Cosmochimica Acta, v. 103, p. 11–25, https://doi.org/10.1016/j.gca.2012.10.014.

Ling, H.F., Jiang, S.Y., Frank, M., Zhou, H.Y., Zhou, F., Lu, Z.L., Chen, X.M., Jiang, Y.H., and Ge, C.D., 2005, Differing controls over the Cenozoic Pb and Nd isotope evolution of deepwater in the central North Pacific Ocean: Earth and Planetary Science Letters, v. 232, p. 345–361, https://doi.org/10.1016/j.epsl.2004.12.009.

McArthur, J.M., Howarth, R.J., and Bailey, T.R., 2001, Strontium isotope stratigraphy: LOWESS version 3: Best fit to the marine Sr-isotope curve for 0–509 Ma and accompanying look-up table for deriving numerical age: The Journal of Geology, v. 109, p. 155–170, https://doi.org/10.1086/319243.

Misra, S., and Froelich, P.N., 2012, Lithium isotope history of Cenozoic seawater: Changes in silicate weathering and reverse weathering: Science, v. 335, p. 818–823, https://doi.org/10.1126/science.1214697.

Nielsen, S.G., Mar-Gerrison, S., Gannoun, A., LaRowe, D., Klemm, V., Halliday, A.N., Burton, K.W., and Hein, J.R., 2009, Thallium isotope evidence for a permanent increase in marine organic carbon export in the early Eocene: Earth and Planetary Science Letters, v. 278, p. 297–307, https://doi.org/10.1016/j.epsl.2008.12.010.

Ravizza, G., and Peucker-Ehrenbrink, B., 2003, The marine [187]Os/[188]Os record of the Eocene–Oligocene transition: The interplay of weathering and glaciation: Earth and Planetary Science Letters, v. 210, p. 151–165, https://doi.org/10.1016/S0012-821X(03)00137-7.

Reifenröther, R., Münker, C., Paulick, H., and Scheibner, B., 2022, Alteration of abyssal peridotites is a major sink in the W geochemical cycle: Geochimica et Cosmochimica Acta, v. 321, p. 35–51, https://doi.org/10.1016/j.gca.2021.12.030.

Roué, L., Kurzweil, F., Wille, M., Wegwerth, A., Dellwig, O., Münker, C., and Schoenberg, R., 2021, Stable W and Mo isotopic evidence for increasing redox-potentials from the Paleoarchean towards the Paleoproterozoic deep Ocean: Geochimica et Cosmochimica Acta, v. 309, p. 366–387, https://doi.org/10.1016/j.gca.2021.05.013.

Sen Tuna, G., and Braida, W., 2014, Evaluation of the adsorption of mono- and polytungstates onto different types of clay minerals and Pahokee peat: Soil and Sediment Contamination, v. 23, p. 838–849, https://doi.org/10.1080/15320383.2014.809049.

Tagliabue, A., Bowie, A.R., Boyd, P.W., Buck, K.N., Johnson, K.S., and Saito, M.A., 2017, The integral role of iron in ocean biogeochemistry: Nature, v. 543, p. 51–59, https://doi.org/10.1038/nature21058.

Teng, F.Z., Dauphas, N., and Watkins, J.M., 2017, Non-traditional stable isotopes: Retrospective and prospective: Reviews in Mineralogy and Geochemistry, v. 82, p. 1–26, https://doi.org/10.2138/rmg.2017.82.1.

Tsujisaka, M., Nishida, S., Takano, S., Murayama, M., and Sohrin, Y., 2020, Constraints on redox conditions in the Japan Sea in the last 47,000 years based on Mo and W as palaeoceanographic proxies: Geochemical Journal, v. 54, p. 351–363, https://doi.org/10.2343/geochemj.2.0606.

van de Flierdt, T., Frank, M., Halliday, A.N., Hein, J.R., Hattendorf, B., Günther, D., and Kubik, P.W., 2004, Tracing the history of submarine hydrothermal inputs and the significance of hydrothermal hafnium for the seawater budget—A combined Pb–Hf–Nd isotope approach: Earth and Planetary Science Letters, v. 222, p. 259–273, https://doi.org/10.1016/j.epsl.2004.02.025.

Westerhold, T., et al., 2020, An astronomically dated record of Earth's climate and its predictability over the last 66 million years: Science, v. 369, p. 1383–1387, https://doi.org/10.1126/science.aba6853.

Yang, R.Y., Li, T., Stubbs, D., Chen, T.Y., Liu, S., Kemp, D.B., Li, W.Q., Yang, S.Y., Chen, J.F., Elliott, T., Dellwig, O., Chen, J., and Li, G.J., 2022, Stable tungsten isotope systematics on the Earth's surface: Geochimica et Cosmochimica Acta, v. 322, p. 227–243, https://doi.org/10.1016/j.gca.2022.01.006.

Yao, W.Q., and Paytan, A., 2020, Possible triggers of the seawater sulfate S-isotope increase between 55 and 40 million years ago: Chemical Geology, v. 552, https://doi.org/10.1016/j.chemgeo.2020.119788.

Yao, W.Q., Paytan, A., Griffith, E.M., Martínez-Ruiz, F., Markovic, S., and Wortmann, U.G., 2020, A revised seawater sulfate S-isotope curve for the Eocene: Chemical Geology, v. 532, https://doi.org/10.1016/j.chemgeo.2019.119382.